Hindawi
Advances in Civil Engineering
Volume 2018, Article ID 5426731, 9 pages
https://doi.org/10.1155/2018/5426731

Research Article

Tests of Inclined Concrete-Filled Steel Tubular Stub Columns under Vertical Cyclic Loading

Chayanon Hansapinyo,[1] **Chinnapat Buachart**,[1] **and Preeda Chaimahawan**[2]

[1]*Excellence Center in Infrastructure Technology and Transportation Engineering (ExCITE), Chiang Mai University, Chiang Mai, Thailand*
[2]*School of Engineering, University of Phayao, Phayao, Thailand*

Correspondence should be addressed to Chayanon Hansapinyo; chayanon@eng.cmu.ac.th

Received 30 June 2018; Accepted 26 July 2018; Published 2 September 2018

Academic Editor: Tadeh Zirakian

This paper presents an experimental study on the cyclic behavior of fifteen concrete-filled steel tubular columns subjected to vertical cyclic loading. All test samples' cross-sectional area is 75×75 mm^2 square, and they are 500 mm long. The main variables in the test are the thickness of the steel tube (1.8 and 3.0 mm with the width-to-thickness ratios (b/t) of 41.7 and 25), the strength of the infilled concrete (no-fill, 23 MPa, and 42 MPa), and the inclined angle (0, 4, and 9 degrees). The results show that all samples failed due to local buckling in compression followed by tearing of the steel tube in tension. The inclination angles of 4 and 9 degrees decreased the vertical compressive capacity of the 1.8 mm vertical hollowed steel column by 34 and 39 percent, respectively. However, the infilled concrete and thicker tube (3.0 mm) could substantially reduce the adverse effect of the inclination angle. The compressive ductility of the hollowed column with the thinner tube was significantly enhanced by the infilled concrete as well.

1. Introduction

A number of buildings and structures have been constructed not only to achieve the functional purpose but also to acquire an aesthetic purpose. Hence, for an architectural reason, buildings with irregularity have been frequently designed such as dome, arch, slender, and inclined columns. For the construction of such structures, steel becomes popular as the high ratio in strength-to-weight characteristic minimizes the negative effect of the mass in the irregular buildings. In addition, its reliable material properties, easy construction procedure, and time efficiency have made the steel more widely adopted. In general, steel performs well under tensile force and gives a ductile manner which is desirable for the seismic resistance design. However, it performs quite poor under compression load with the increase of slenderness. Especially for thin-wall steel member, the local buckling is possibly formed and eventually failed before it reaches the yield point. This undesirable mechanism causes the strength reduction in steel structures.

To enhance the compressive loading capacity, sectional stiffeners with additional lips are included for the thin-wall steel open sections [1]. For the hollow section, filling of the concrete inside is the most popular solution. It is well recognized that the concrete-filled steel tube column (hereinafter, CFST column) provides an outstanding behavior not only loading capacity but also an admirable durability. The steel hollow section performs as casting form and reinforcement. Furthermore, the CFST column also helps reduce construction time due to its construction simplicity. With the benefits of the CFST columns, using of the columns becomes widely adopted for multistorey building construction [2] and bridge piers [3]. In addition, the CFST columns also offer the advantage of preventing progressive collapse of buildings under blast loading [4]. However, there are some complications in the calculation of its capacity. Estimation of loading capacity of the CFST column is not just a direct superposition of the individual capacity of the infilled concrete and the hollow steel. The combination of the materials results to confinement of the infilled concrete and buckling prevention of the thin-wall steel. Hence, many previous researches focused on determination of parameters affecting the interaction. Schneider [5] conducted an experimental and analytical

study on the behavior of short, concrete-filled steel tube columns concentrically loaded in compression to failure. The effect of thickness, length, and section dimension of the CFST column on the concrete confinement, bearing capacity, and ductility was addressed. With the advancement in materials, the effect of high material strength was investigated by Liu et al. [6] and Zhou et al. [7]. Using of carbon fiber reinforced polymer (CFRP) to confine the CFST columns was investigated by Guo and Zhang [8]. The study indicated the increase of confinement using the outer CFRP especially for the square column. The effect of heat on the CFRP-confined CFST column was investigated by Chen et al. [9].

For loading capacity prediction and code comparisons, Han et al. [10] proposed a mechanic model based on a series of CFST column tests considering the composite action. The predicted load-deflection relationship conformed with the test results. A nonlinear finite element numerical model was adopted by Abed et al. [11] to predict compressive behavior of CFST columns. The study indicated the effect of diameter-to-thickness ratio (D/t) as the main variable governing the compressive behavior. The underestimation of the axial capacity calculated by design codes, for example, AISC, ACI318, AS, and EC4, reduces as the D/t ratio increases. Liu et al. [6] found that unequal widths of the two sides of concrete-filled rectangular hollow section led to poor performance in bearing capacity and ductility. Hence, square section was suitable for the CFST column. Regarding the comparison of loading capacity with design codes, EC4 gave a close prediction with 6% difference. For other codes, AISC and ACI codes underestimated the ultimate load by 16% and 14%, respectively.

Most of the studies focused on stub columns. Buckling of slender CFST columns was investigated by Ruoquan [12], Vrcelj and Uy [13], and Goode et al. [14]. The study indicated the accuracy of the bearing capacity using methods presented by EC4. The benefit of using the CFST columns in seismic is also appreciated. Under seismic loading, the CFST performed very well as confirmed by cyclic load tests and analyses conducted by Hansapinyo [15], Abdalla et al. [16], Mao and Xiao [17], and Buachart et al. [18]. Due to the buckling restraint, ductility and energy dissipation capacity are increased.

The more complicated behavior can be seen when the CFST is subjected to combined axial and bending loading or when the loading is not aligned with the member axis. These situations can be easily found for an irregular structural arrangement in a building. Figure 1 shows schematic view of inclined CFST column application in buildings. Opened view, long span, and unique style building can be achieved. However, only a few researches discussed about the loading capacity of the inclined CFST column. Han et al. [19] experimentally investigated the influence of the angle of inclination and tapered CFST columns under compressive loading. It was found that the increase of the inclined angle tended to reduce the bearing capacity of the column. Failure patterns of hollow steel section were both inward and outward buckling. In the CFST columns, only outward buckling could be observed as a result of the constraining effect provided by the infilled concrete.

Although many researches have been conducted in the field of CFST columns, there have been only a few studies on the behavior of inclined CFST columns under cyclic loading. Therefore, this study was aimed to analyse the behavior of inclined CFST columns when subjected to cyclic loading. Fifteen CFST columns were tested under vertical cyclic load until they reach the state of failure. The effect of inclination angle, concrete strength, and wall thickness on the loading capacity, ductility, and energy dissipation is discussed.

2. Experimental Works

2.1. Samples and Experimental Setup. A total of 15 samples were experimentally examined in this study. For all samples, the cross-sectional depth (b) is $75 \times 75\,\text{mm}^2$ and the length (l) is 500 mm. The length-to-depth ratio (l/b) is 6.67, enabling the prevention of overall column buckling. The variables in this test are the infilled concrete strength, thickness of the steel tube, and the inclination angle, as shown in Table 1. The sample nomenclature is defined to identify three investigated parameters. The initial letter "T" stands for the thickness of the steel tube. The second letter "C" stands for the designed cylindrical compressive strength of the infilled concrete, and the last letter "A" stands for the inclination angle of the tested samples. For example, the sample with label of T1.8C20A4 indicates the sample with the thickness of steel tube of 1.8 mm, filled with designed 20 MPa concrete, and the inclination angle is 4 degrees. It is noted that the compressive strength was tested for 28-day compressive strength which were 23 and 42 MPa, respectively, for the targeted 20 and 40 MPa concretes. A coupon tensile test was made to determine the yielding and the ultimate tensile strength of the steel tubes. The yield strength was 264 and 382 MPa for T1.8 and T3.0, respectively. The ultimate strength was 305 and 441 MPa for T1.8 and T3.0, respectively. Based on EC4 [20], for the local buckling resistance design, the maximum limit of the width-to-thickness ratios (b/t) is calculated using (1). For samples with 1.8 mm and 3 mm thick steel tube, the ratios are about 41.7 and 25, which are, respectively, below the limits of 49.1 and 40.9. For a CFST member, the potential of local buckling is estimated using a width-to-thickness ratio parameter R [21] as shown in (2). In the equations, f_y, E, and ν are yield strength, elastic modulus, and Poisson's ratio of steel, and k is the buckling coefficient, $k = 4n^2$, where $n = 1$ and 2 for unstiffened section and stiffened section with one stiffener on each wall. For the composite column with the thickness of 1.8 and 3.0 mm, the parameter R is 0.80 and 0.58, respectively, which is lower than the limit of 0.9 [21].

$$\frac{b}{t} = 52\sqrt{\frac{235}{f_y}}, \tag{1}$$

$$R = \frac{b}{t}\sqrt{\frac{12\left(1-\nu^2\right)}{\pi^2 k}}\sqrt{\frac{f_y}{E}}. \tag{2}$$

Other important factors for the composite column design are the steel contribution ratio (δ) and confinement factor (ξ), which are expressed in (3) and (4), respectively.

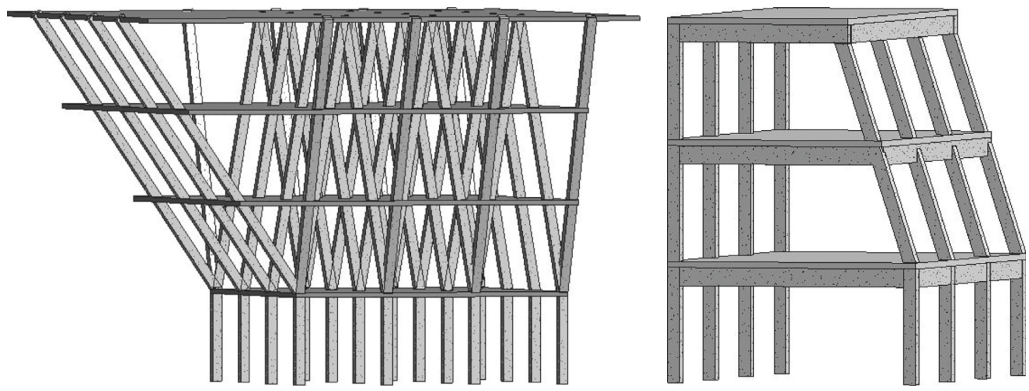

(a) (b)

Figure 1: Example of application of inclined column.

Table 1: Samples.

Number	Sample	B (mm)	T (mm)	θ (deg)	b/t	R	f'_c (MPa)	δ	ξ	N_{cu} (kN)	SI_c	N_{tu} (kN)	SI_t
1	T1.8C0A0	75	1.8	0	41.7	—	—	1	—	150.0	1.00	150.7	1.00
2	T1.8C0A4	75	1.8	4	41.7	—	—	1	—	99.0	0.66	150.6	1.00
3	T1.8C0A9	75	1.8	9	41.7	—	—	1	—	91.1	0.61	150.5	1.00
4	T1.8C20A0	75	1.8	0	41.7	0.80	23	0.56	1.30	268.2	1.00	162.4	1.00
5	T1.8C20A4	75	1.8	4	41.7	0.80	23	0.56	1.30	260.0	0.97	163.4	1.01
6	T1.8C20A9	75	1.8	9	41.7	0.80	23	0.56	1.30	253.3	0.94	162.2	1.00
7	T1.8C40A0	75	1.8	0	41.7	0.80	42	0.42	0.71	413.8	1.00	152.8	1.00
8	T1.8C40A4	75	1.8	4	41.7	0.80	42	0.42	0.71	334.5	0.81	192.5	1.26
9	T1.8C40A9	75	1.8	9	41.7	0.80	42	0.42	0.71	327.8	0.79	164.5	1.08
10	T3.0C0A0	75	3.0	0	25.0	—	—	1	—	340	1.00	345	1.00
11	T3.0C0A4	75	3.0	4	25.0	—	—	1	—	330	0.97	342.4	0.99
12	T3.0C0A9	75	3.0	9	25.0	—	—	1	—	325.9	0.96	309.1	0.90
13	T3.0C20A0	75	3.0	0	25.0	0.57	23	0.76	3.13	436.5	1.00	350.2	1.00
14	T3.0C20A4	75	3.0	4	25.0	0.57	23	0.76	3.13	427.9	0.98	342.4	0.98
15	T3.0C20A9	75	3.0	9	25.0	0.57	23	0.76	3.13	343.7	0.79	326	0.93

Note. N_{cu} and N_{tu} are, respectively, the ultimate loading capacity under compression and tension. SI_c and SI_t are, respectively, the strength index under compression and tension (6).

The simplified design of the composite column, according to EC4 [20] and ACI318 [22], assumes the plastic resistance of the column composite section under compressive load (N_0) by the sum of the resistances of the concrete and steel. With the assumption, the steel contribution ratio (δ) is limited between 0.2 and 0.9. The ratios of the test composite samples are ranged from 0.42 to 0.76 as shown in Table 1. Hence, they meet the requirement.

$$\delta = \frac{f_y A_s}{N_0} = \frac{f_y A_s}{0.85 f'_c A_c + f_y A_s}, \tag{3}$$

$$\xi = \frac{f_y A_s}{0.85 f'_c A_c}. \tag{4}$$

In preparation of the CFST columns, fresh concrete was filled into the steel tubular section. During the casting, fresh concrete was vibrated. Then, the CFST columns were kept in the curing process for at least 28 days. Thereafter, the CFST samples were welded to end plates and stiffeners at both ends as illustrated in Figure 2. The end plates were holed in the position for bolting to the loading machine. Two stiffeners were welded to the column ends along the inclined center line to increase the joint welding strength under tension and control the in-plane bending. Consequently, the sample was put into a universal testing machine (200 tons) and all testing conditions were set, including strain gauges and transducers in 2 horizontal directions and 1 vertical direction as shown in Figure 2.

2.2. Cyclic Load Test. The test column was arranged in the loading machine as an inclined column in nonsway structure, and the boundary conditions are specified as illustrated in Figure 3. At both ends, samples were restrained in horizontal (x, y), vertical (z), and rotation (r) movement. The inclination generates more complex acting force compared to the concentric axial loading. It can be seen that all forces, including bending, shearing, and compressive or tensile forces, are at both ends of the column. Larger inclination angle introduces higher eccentricity leading to high eccentric bending moment. In a condition when a member is inclined appreciably, shear is found to be predominant and shear capacity demand should be strictly considered. The cyclic vertical load was applied on the top of the samples. As

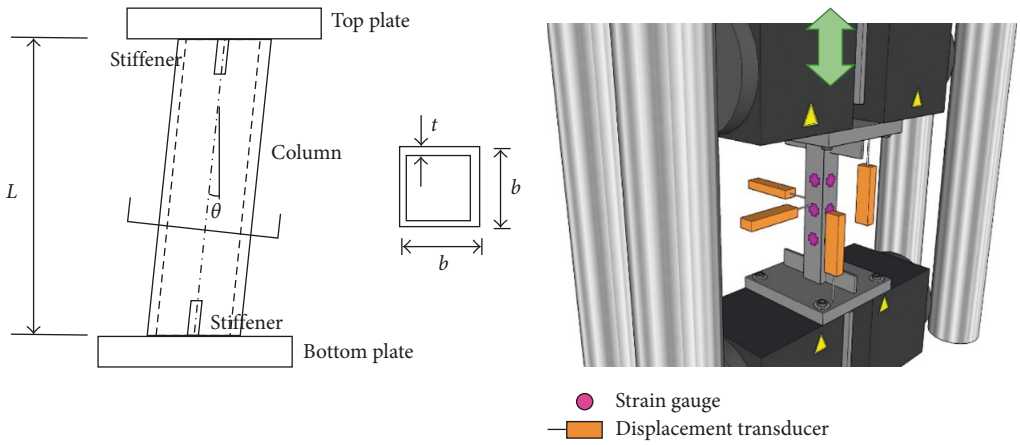

Figure 2: CFST column sample and instrumental setup.

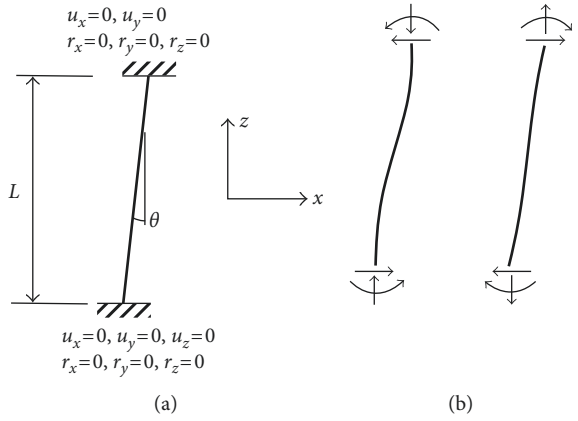

Figure 3: Boundary conditions and induced column forces.

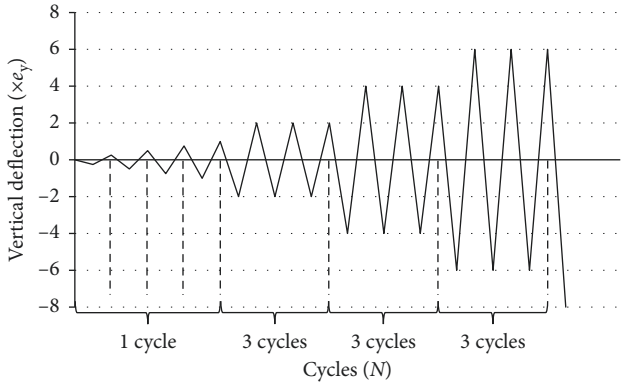

Figure 4: The cyclic load pattern.

a result, the samples were subjected to both elongation and contraction. The magnitude of each cycle was specified using the percentage of the estimated deformation at yield point (e_y) as shown in the following equation:

$$e_y = \frac{f_y}{E} \times L, \tag{5}$$

where e_y is the estimated vertical deformation at yield point, f_y is the yield strength (MPa), E is the modulus of elasticity of the steel tube (MPa), and L is the total length of the sample (mm). The cyclic load pattern can be divided into 2 parts. At initial step before the expected yielding, a series of single-cycle load of $0.25e_y$, $0.50e_y$, $0.75e_y$, and $1.00e_y$ was applied. Thereafter, a series of three-cycle load of $2.0e_y$, $4.0e_y$, $6.0e_y$, and $8.0e_y$ continued to be applied (Figure 4). The samples were tested until they reached the failure state.

3. Experimental Results

3.1. Failure Mode and Axial Load Capacity. Under the incremental increase of the cyclic load as shown in Figure 4, all the samples behaved linearly at the early loading stage. With the larger applied cyclic deformation, local buckling appeared under compressive loading, followed by tension yielding and tearing of the steel tube at the same column section. The yielding and steel tearing led to the complete loss of load bearing capacity. The samples without the infilled concrete were first damaged due to local buckling under the compressive loading, leading to drastic decrease of compressive capacity. With the increase of displacement loading, tension yielding at the local buckling section was generated, but the tension capacity was maintained until the tearing of the tube. However, for the CFST column (with the infilled concrete), major buckling of the steel tube occurred after the tensile yielding. The inclination angle decreases the vertical cyclic compressive loading capacity of the hollowed steel column with thinner wall ($t = 1.8$ mm, $b/t = 41.7$). The strength index under compressive loading (SI_c) indicating the effect of the inclination angle as calculated by (6) is 0.66 and 0.61, respectively, for the 4-degree and 9-degree inclined columns, as shown in Table 1 and Figure 5. However, the inclination angles of 4 and 9 degrees insignificantly reduced the vertical loading capacity of the hollowed columns with thicker wall ($t = 3.0$ mm; $b/t = 25$). The strength index of the two columns is 0.97 and 0.96, respectively. Hence, it can be said that the local buckling capacity of the slender wall

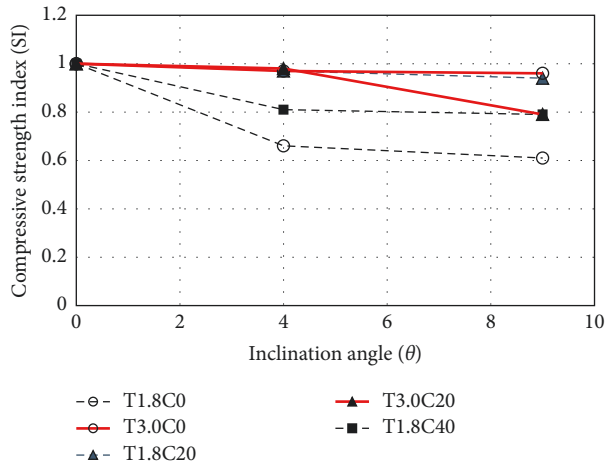

Figure 5: Compressive strength index due to inclination angle.

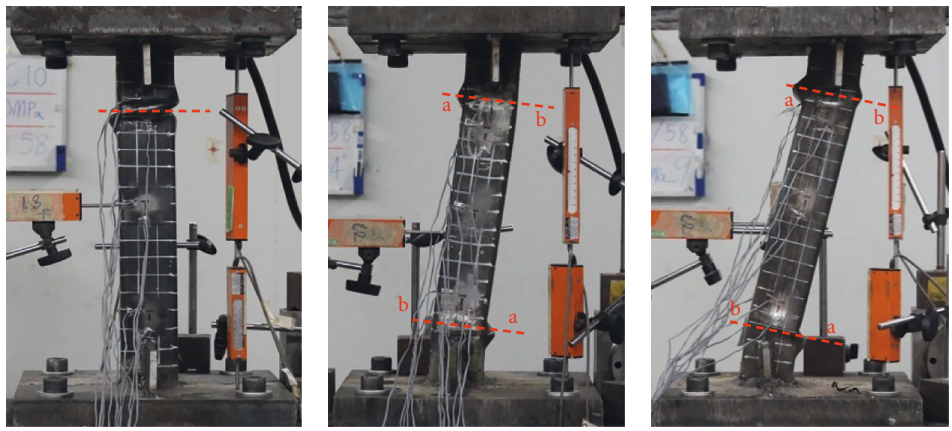

(a) (b) (c)

Figure 6: Failure pattern of T3.0C20 series samples. (a) T3.0C20A0. (b) T3.0C20A4. (c) T3.0C20A9.

hollowed steel column is significantly affected by the inclination angle. For the CFST columns, local compressive buckling was restrained, and hence, they experienced only outward local buckling. Hence, the CFST columns could carry more compressive loads after local buckling. Infilled concrete reduced negative effect of inclination angle is shown in Figure 5. The ultimate compressive loading capacity of the column was obtained when the confined steel walls suffered large tensile strain and torn. At this loading stage, concrete core confinement was decreased and concrete crushing was observed. As an example, Figure 6 shows the failure of T3.0C20 series samples. It can be seen that the local buckling plane shown as the broken line was formed in a direction perpendicular to the longitudinal direction. The inclination leading to end eccentricity results to nonuniform longitudinal compressive stress. As shown in Figure 6 for the T3.0C20 series samples, buckling was more severe on the face with higher compression (face "a") compared with the opposite face (face "b").

$$\mathrm{SI} = \frac{N_{\mathrm{u,inc}}}{N_{\mathrm{u,ver}}}, \tag{6}$$

where SI is the strength index. $N_{\mathrm{u,inc}}$ and $N_{\mathrm{u,ver}}$ are the ultimate strength of inclined and vertical samples, respectively.

3.2. Cyclic Behaviors and Hysteretic Loop. The hysteretic loops of all samples are shown in Figure 7. The hysteretic loops illustrate that the columns performed in the elastic manner at the initial stage of the test. The tensile loading capacity was maintained after the peak for all samples. In the cases of hollow steel columns, the compressive strength was much lower than those in CFST columns and the strength dropped drastically after the compressive peak load. Under the tension side, the infilled concrete and the inclination insignificantly influenced the tension-resisting behavior.

From Figure 7, the hysteretic loop of the infilled concrete columns under compression is more stable compared with those of the unfilled columns. The compressive capacity gradually decreased after the peak compressive load. This desirable behavior leads to higher ductility which will be explained in Section 3.3. The inclination angle delays the sudden drop of the compressive strength after the peak

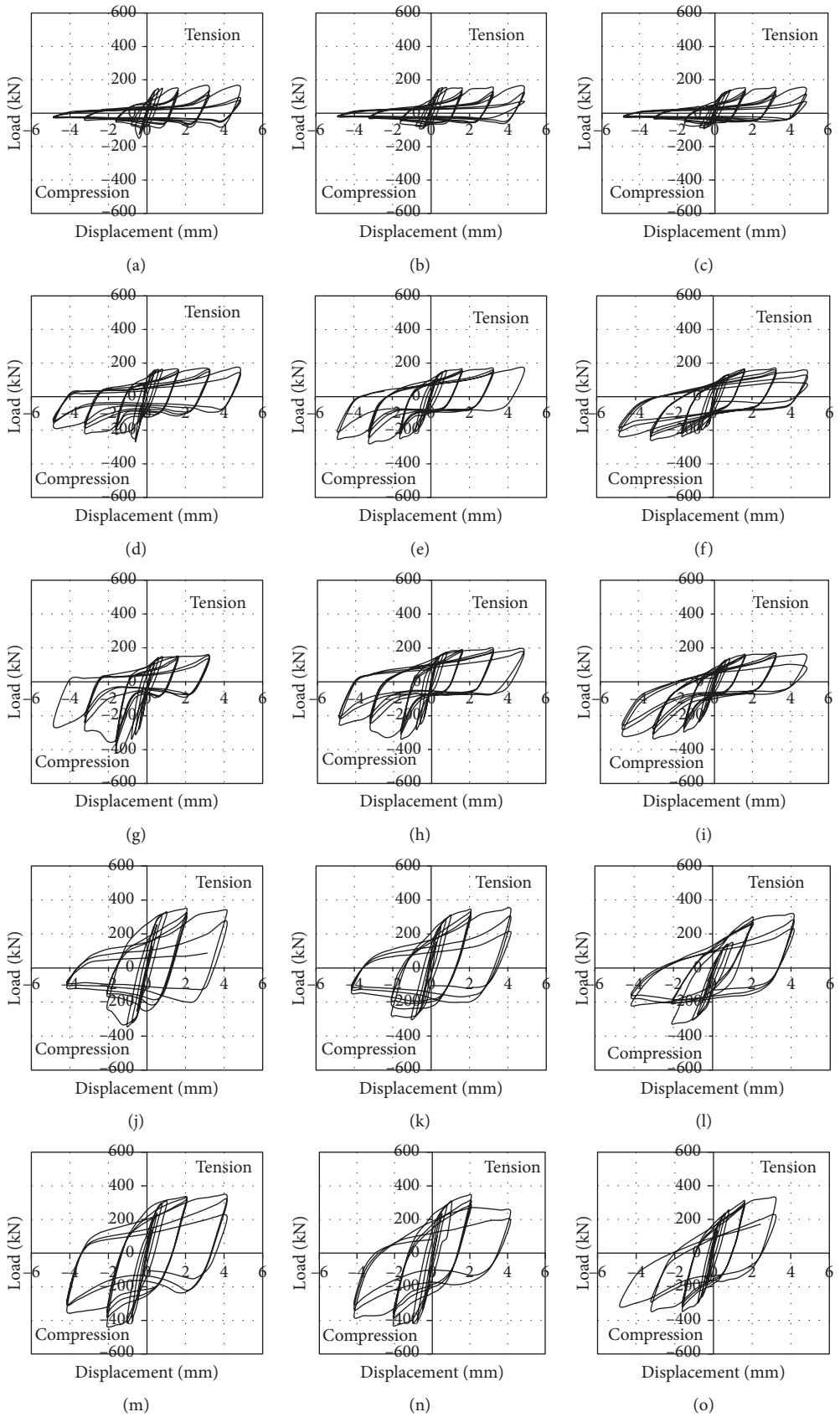

Figure 7: Hysteretic loop. (a) T1.8C0A0. (b) T1.8C0A4. (c) T1.8C0A9. (d) T1.8C20A0. (e) T1.8C20A4. (f) T1.8C20A9. (g) T1.8C40A0. (h) T1.8C40A4. (i) T1.8C40A9. (j) T3.0C0A0. (k) T3.0C0A4. (l) T3.0C0A9. (m) T3.0C20A0. (n) T3.0C20A4. (o) T3.0C20A9.

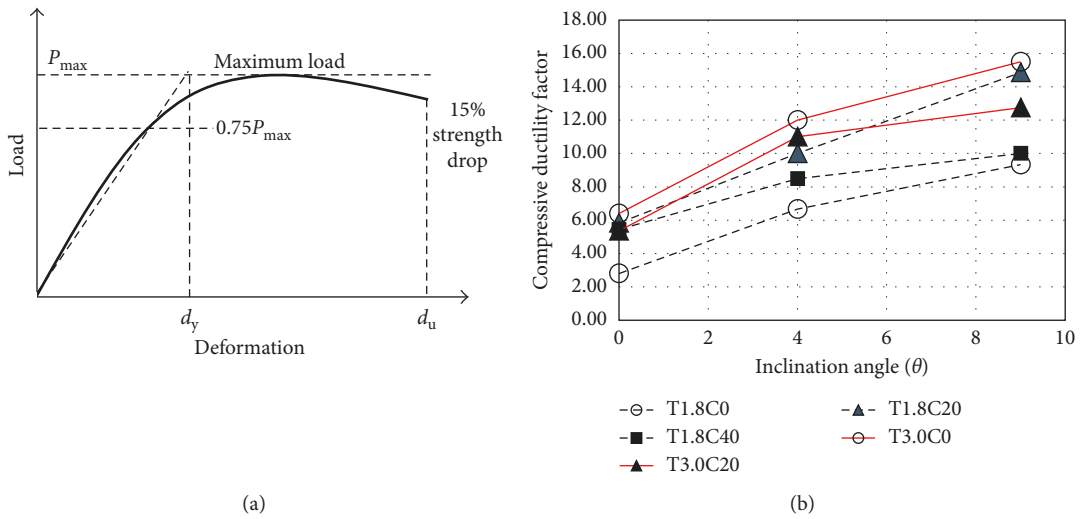

(a) (b)

Figure 8: Ductility factor. (a) Determination of the ductility factor. (b) Compressive ductility factor of the samples.

Table 2: Ductility factor and equivalent viscous damping.

Number	Sample	Ductility in compression			Ductility in tension			Equivalent viscous damping ratio	
		d_y (mm)	d_u (mm)	μ (deg)	d_y (mm)	d_u (mm)	μ (deg)	Elastic	Inelastic
1	T1.8C0A0	0.25	0.70	2.80	0.30	5.10	17.00	6.5	25.1
2	T1.8C0A4	0.15	1.00	6.67	0.25	4.75	19.00	7.3	23.2
3	T1.8C0A9	0.15	1.40	9.33	0.25	4.90	19.60	4.5	22.2
4	T1.8C20A0	0.6	3.5	5.83	0.2	4.5	22.50	6.9	26.0
5	T1.8C20A4	0.5	5.0	10.00	0.15	5	33.33	5.2	23.1
6	T1.8C20A9	0.35	5.2	14.86	0.15	4.85	32.33	5.9	24.7
7	T1.8C40A0	0.45	2.45	5.44	0.35	2.75	7.86	5.2	14.4
8	T1.8C40A4	0.5	4.25	8.50	0.3	4.6	15.33	5.2	23.6
9	T1.8C40A9	0.5	5.0	10.00	0.3	4.85	16.17	5.7	15.7
10	T3.0C0A0	0.25	1.60	6.40	0.30	4.20	14.00	3.5	24.4
11	T3.0C0A4	0.10	2.4	12.00	0.15	4.15	27.67	3.3	26.3
12	T3.0C0A9	0.20	3.1	15.50	0.15	4.10	27.33	4.1	25.2
13	T3.0C20A0	0.7	3.75	5.36	0.4	4.1	10.25	6.2	28.7
14	T3.0C20A4	0.4	4.4	11.00	0.5	3.5	7.00	4.8	25.5
15	T3.0C20A9	0.4	5.1	12.75	0.4	2.95	7.38	2.3	22.7

because the inclination angle decreases the ultimate compressive loading capacity and results to higher ductility.

3.3. Ductility and Equivalent Viscous Damping Ratio. The ductility determines the ability of a structure to maintain the load carrying capacity after the commencement of yielding to the ultimate displacement. Park [23] proposed the definition of ductility factor (μ) as the ratio of the equivalent yield displacement (d_y) to the ultimate displacement (d_u). As shown in Figure 8(a), the backbone curves of all samples are drawn, and the ductility factor can be determined. The results are shown in Table 2 and Figure 8(b) which indicates that the inclination angle increases the ductility under compression loading. The smallest compressive ductility factor of 2.8 is from T1.8C0A0, the unfilled thin steel tube column with zero inclination angle. Filling of lower strength concrete (23 MPa) in the thin hollow steel column can enhance the ductility factor from 2.80 to 5.83. However, the thinner section filled with higher concrete compressive strength may result in the substantial increase of strength but less efficient in ductility enhancement.

The equivalent viscous damping ratio (ζ_{eq}) indicates energy dissipation capacity during inelastic response. The estimation of the ratio expressed by Chopra [24] was implemented in this study, as shown in (7). In the elastic range, the equivalent viscous damping ratios of all of the samples are in the range of 2.3–7.3%. The values are between 14.4 and 28.7 in the inelastic range. The inclination angle seems to have no effect on the ratio, as shown in Figure 9(b). The infilled high strength concrete (42 MPa) tends to decrease the damping ratio of the thinner CFST columns.

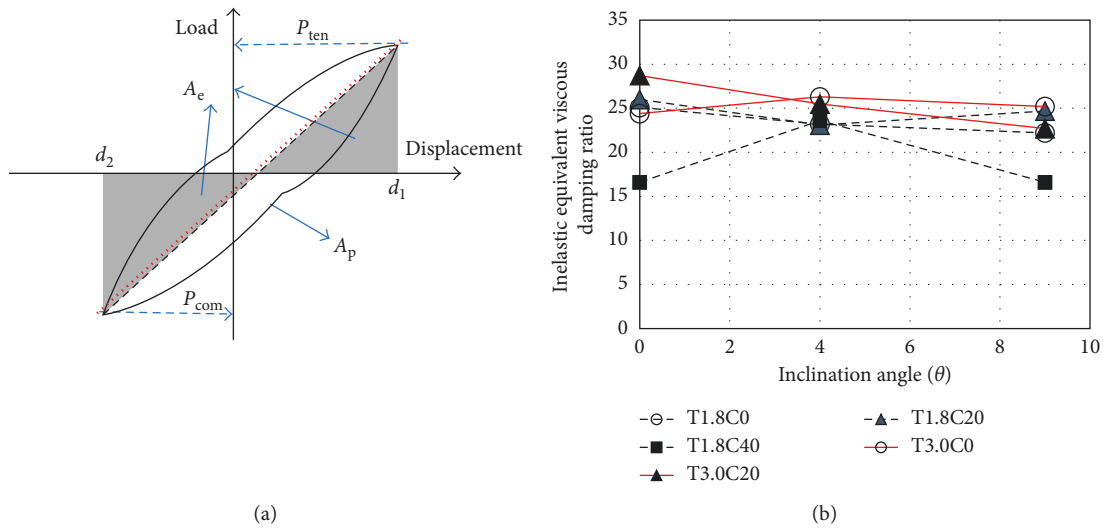

(a) (b)

Figure 9: Equivalent viscous damping ratio. (a) Determination of the equivalent viscous damping ratio. (b) Equivalent viscous damping ratio of the samples.

$$\zeta_{eq} = \frac{1}{2\pi}\frac{A_p}{A_e} \times 100. \quad (7)$$

4. Conclusions

In this paper, CFST inclined columns were tested under vertical cyclic load. From the test results, the following conclusions can be drawn:

(1) The local buckling capacity of the slender wall hollowed steel column is significantly affected by the inclination angle. The strength index (SI) under compressive loading of T1.8C0 samples is 0.66 and 0.61, respectively, for the 4-degree and 9-degree inclined columns. However, the inclination angles of 4 and 9 degrees insignificantly reduced the vertical loading capacity of the hollowed columns with thicker wall ($t = 3.0$ mm, $D/t = 25$). The strength index of the columns is 0.97 and 0.96, respectively.

(2) The infilled concrete enhanced the compressive cyclic behavior of the steel hollow section. For the ductility, filling of lower strength concrete (23 MPa) in the thin hollow steel column can enhance the ductility factor from 2.80 (T1.8C0A0 sample) to 5.83 (T1.8C20A0 sample). However, the thinner section filled with higher concrete compressive strength may result to the substantial increase of strength but less efficient in ductility enhancement. The inclination angle decreases the ultimate compressive loading capacity and results to the higher ductility.

(3) For the equivalent viscous damping ratio, the values of all samples are between 14.4 and 28.7 in the inelastic range. The inclination angle seems to have no effect on the ratio. The infilled high strength concrete (42 MPa) tends to decrease the damping ratio of the thinner CFST columns.

Data Availability

The data used to support the findings of this study are included within the article.

Conflicts of Interest

The authors declare that there are no conflicts of interest regarding the publication of this paper.

Acknowledgments

The authors would like to acknowledge the supports provided by Chiang Mai University.

References

[1] C. Hansapinyo, "Buckling performance of irregular section cold-formed steel columns under axially concentric loading," *International Journal of Civil, Structural, Construction and Architectural Engineering*, vol. 9, no. 5, pp. 542–548, 2015.

[2] J. Y. R. Liew and D. X. Xiong, "Ultra-high strength concrete filled composite columns for multi-storey building construction," *Advances in Structural Engineering*, vol. 15, no. 9, pp. 1487–1503, 2012.

[3] R. Yadav, B. Chen, H. Yuan, and Z. Lian, "Analytical behavior of CFST bridge piers under cyclic loading," *Procedia Engineering*, vol. 173, pp. 1731–1738, 2017.

[4] J. Zhang, S. Jiang, B. Chen, C. Li, and H. Qin, "Numerical study of damage modes and damage assessment of CFST columns under blast loading," *Shock and Vibration*, vol. 2016, Article ID 3972791, 12 pages, 2016.

[5] S. P. Schneider, "Axially loaded concrete-filled steel tubes," *Journal of Structural Engineering*, vol. 124, no. 10, pp. 1125–1138, 1998.

[6] D. Liu, W. M. Gho, and J. Yuan, "Ultimate capacity of high-strength rectangular concrete-filled steel hollow section stub columns," *Journal of Constructional Steel Research*, vol. 59, no. 12, pp. 1499–1515, 2003.

[7] X. Zhou, T. Mou, H. Tang, and B. Fan, "Experimental study on ultrahigh strength concrete filled steel tube short columns

under axial load," *Advances in Materials Science and Engineering*, vol. 2017, Article ID 8410895, 9 pages, 2017.

[8] Y. Guo and Y. Zhang, "Comparative study of CFRP-confined CFST stub columns under axial compression," *Advance in Civil Engineering*, vol. 2018, Article ID 7109061, 8 pages, 2018.

[9] Y. Chen, K. Wang, K. He, J. Wei, and J. Wan, "Compressive behavior of CFRP-confined post heated square CFST stub columns," *Thin-Walled Structures*, vol. 127, no. 6, pp. 434–445, 2018.

[10] L. H. Han, X. L. Zhao, and Z. Tao, "Tests and mechanics model of concrete-filled SHS stub columns, columns and beam-columns, steel and composite structures," *Steel and Composite Structures*, vol. 1, no. 1, pp. 51–74, 2001.

[11] F. Abed, M. Alhamaydeh, and S. Abdalla, "Experimental and numerical investigations of the compressive behavior of concrete filled steel tubes (CFSTs)," *Journal of Constructional Steel Research*, vol. 80, no. 1, pp. 429–439, 2013.

[12] H. Ruoquan, "Behaviour of long concrete filled steel columns, composite construction in steel and concrete II," in *Proceedings of Engineering Foundation Conference*, pp. 728–737, Santa Barbara, CA, USA, June 1992.

[13] Z. Vrcelj and B. Uy, "Strength of slender concrete-filled steel box columns incorporating local buckling," *Journal of Constructional Steel Research*, vol. 58, no. 2, pp. 275–300, 2002.

[14] C. D. Goode, A. Kuranovas, and A. K. Kvedaras, "Buckling of slender composite concrete-filled steel columns," *Journal of Civil Engineering and Management*, vol. 16, no. 2, pp. 230–237, 2010.

[15] C. Hansapinyo, "Responses of concrete-filled cold-formed square hollow and double-C steel stub columns under cyclic and repeated loadings," *Advanced Materials Research*, vol. 255–260, pp. 198–203, 2011.

[16] S. Abdalla, F. Abed, and M. Alhamaydeh, "Behavior of CFSTs and CCFSTs under quasi-static axial compression," *Journal of Constructional Steel Research*, vol. 90, no. 11, pp. 235–244, 2013.

[17] X. Y. Mao and Y. Xiao, "Seismic behaviour of confined square CFT columns," *Engineering Structures*, vol. 63, no. 3, pp. 317–325, 2007.

[18] C. Buachart, C. Hansapinyo, and N. Ueatrongchitt, "Analysis of square concrete-filled cold-formed steel tubular columns under axial cyclic loading," *International Journal of GEOMATE*, vol. 15, no. 47, pp. 74–80, 2018.

[19] L. H. Han, Q. X. Ren, and W. Li, "Test on inclined, tapered and STS concrete-filled steel tubular (CFST) stub columns," *Journal of Constructional Steel Research*, vol. 66, no. 10, pp. 1186–1195, 2010.

[20] Eurocode 4, *Design of Composite Steel and Concrete Structures, Part 1.1, General Rules and Rules for Building*, BS EN1994-1-1: 2004, British Standards Institution, London, UK, 2004.

[21] H. B. Ge and T. Usami, "Strength analysis of concrete-filled thin-walled steel box columns," *Journal of Constructional Steel Research*, vol. 30, no. 3, pp. 259–281, 1994.

[22] ACI 318, *Building Code Requirements for Structural Concrete and Commentary*, American Concrete Institute, Farmington Hills, MI, USA, 2014.

[23] R. Park, "Evaluation of ductility of structures and structural assemblages from laboratory testing," *Bulletin of the New Zealand National Society for Earthquake Engineering*, vol. 22, no. 3, pp. 155–166, 1989.

[24] A. K. Chopra, *Dynamic of Structures-Theory and Applications to Earthquake Engineering*, Prentice-Hall, Inc., Englewood Cliffs, NJ, USA, 2011.